2023 EELS Field Tests at Athabasca Glacier as an Icy Moon Analogue Environment

Michael Paton[1]*, Richard Rieber[1]*, Sarah Cruz[1]*, Matt Gildner[1], Chantelle Abma[2], Kevin Abma[2], Sina Aghli[1], Eric Ambrose[1], Avak Archanian[1], Elizabeth A. Bagshaw[3], Cathy Baroco[2], Andrew Blackstock[2], Joseph Bowkett[1], Morgan L. Cable[1], Eduardo Cartaya[2], Guglielmo Daddi[1,4], Tomas Drevinskas[1], Rachel Etheredge[1], Tom Gall[2], Alex S. Gardner[1], Peter Gavrilov[1], Nikola Georgiev[1], Katie Graham[2], Benjamin Hockman[1], Bryson Jones[1], Scott Linn[2], Michael J. Malaska[1], Eloïse Marteau[1], Nick Maslen[2], Hovhannes Melikyan[1], Yashwanth Kumar Nakka[1], Jason Nelson, Michele Pazzini[2], Martin Peticco[1], Michael Prior-Jones[5], Matthew Robinson[1], Christiahn Roman[1], Rob Royce[1], Mary Ryan[2], Lori Shiraishi[1], Christian Stenner[2], Marlin Strub[1], Robert Michael Swan[1], Ben Swerdlow[2], Rohan Thakker[1], Luis Phillipe Tosi[1], Tony Tran[1], Tiago Stegun Vaquero[1], Marcel Veismann[1], Tom Wood[2], Harshad Zade[1], Masahiro Ono[1]
authors contributed equally

[1]Jet Propulsion Laboratory California Institute of Technology {mpaton, ono}@jpl.nasa.gov

[2]Direct Action Vertical

[3]University of Bristol

[4]Politecnico di Torino

[5]Cardiff University

Abstract— JPL is developing a versatile and highly intelligent Exobiology Extant Life Surveyor (EELS) robot that would enable access to subsurface oceans and near-surface liquid reservoirs through existing conduits, such as the vents at the south pole of Enceladus or the putative geysers on Europa. A key mobility requirement for future vent exploration missions will be the ability to carefully descend and hold position in the vent to collect and analyze samples while withstanding plume forces without human intervention. Furthermore, this must be accomplished in a highly uncertain environment, requiring versatile hardware and intelligent autonomy. To work towards that goal, we have prototyped the EELS 1.0 and EELS 1.5 robots for horizontal and vertical mobility, respectively, in icy terrain. Autonomous surface mobility of EELS 1.0 was previously validated in a variety of terrain, including snowy mountains, ice rinks, and desert sand. Vertical mobility of EELS 1.5 was developed on laboratory ice walls. This paper presents the first mobility trials for both robots on large-scale, natural icy terrain: the Athabasca Glacier located in Alberta, Canada, a terrestrial analogue to the surfaces and subsurfaces of icy moons. This paper provides a preliminary written record of the test campaign's four major trials: 1) surface mobility with EELS 1.0, 2) vertical mobility with EELS 1.5, 3) science instrument validation, and 4) terramechanics experiments. During this campaign, EELS 1.5 successfully held position and descended ~1.5 m vertically in an icy conduit and EELS 1.0 demonstrated surface mobility on icy surfaces with undulations and slopes. A miniaturized capillary electrophoresis (CE) instrument built to the form factor of an EELS module was tested in flowing water on the glacier and successfully demonstrated automated sampling and in-situ analysis. Terramechanics experiments designed to better understand the interaction between different ice properties and the screws that propel the robot forwards were performed on horizontal and vertical surfaces. In this paper we report the outcomes of the four tests and discuss their implications for potential future icy missions. The field test also demonstrated EELS's ability to support Earth science missions. Another potential near-term follow-on could be a technology demonstration on the Moon. This paper is a high level report on the execution of the field test. Data and results will be detailed in subsequent publications.

TABLE OF CONTENTS

Figure 1: Left - Mission concept illustration of the EELS robot traversing on the surface of an icy moon (top) and descending into a vertical conduit (bottom). Right - EELS 1.0 (top) and EELS 1.5 (bottom) prototype robots conducting mobility trials on the Athabasca Glacier, a terrestrial icy-moon analog. Credit: NASA JPL.

1. INTRODUCTION

Robotic space missions in the past have focused on relatively safe and accessible destinations in the Solar System, such as circumplanetary orbits or the mostly flat terrains on the Moon and Mars. To answer some of the remaining big questions in planetary science and astrobiology, future missions will need to face increasingly challenging environmental conditions, characterized by a substantial level of uncertainty. For example, the Enceladus Vent Explorer (EVE) mission concept [1, 2], which aims to directly sample the subsurface ocean to search for and characterize life, would require a robot to traverse the complex surface of the Enceladus South Pole and climb down an actively erupting vent. The environment in the vent is dynamic [3] and reconnaissance from an orbital-only mission would provide insufficient data at the scale of a robot. Pushing the frontier of discovery into such challenging destinations would require a robotic explorer that is highly versatile and intelligent. An adaptable robot with multiple mobility modes could negotiate a wide range of terrains, some of which may be uncharacterized prior to landing. Such a robot could flexibly accommodate contingencies and make risk-aware decisions while operating in a destination with substantial light-time delay or a limited communication link. The purpose of the ongoing EELS project is to develop and test a robotic system to enable the exploration of previously inaccessible corners of the Solar System.

The Exobiology Extant Life Surveyor (EELS) concept is a snake-like robot that was designed to cleverly address the problem of accessing hard-to-reach subsurface oceans through existing natural terrain features such as the active conduits of Enceladus (Figure 1, left). With biologically inspired motility and highly capable autonomy, the robot can traverse horizontally and vertically on a wide range of surfaces, from ice and snow to rock and loose regolith, along undulating surfaces to crevasses, pits, and subsurface fissures and conduits. The snake-robot design is particularly useful for ocean-world vent exploration due to its ability to resist upward plume forces by expanding outwards against the icy walls while using active-skin propulsion to descend (Figure 1, right). Furthermore, the robot's small axial footprint will enable traversal through centimeter-scale choke points in ocean world vents.

JPL is currently prototyping a suite of EELS robots for testing across various terrestrial analogue environments. Our first prototype, *EELS 1.0*, was developed for *surface mobility* and successfully demonstrated traversal using a variety of gaits in snowy, icy, and sandy field tests in natural, in situ environments in addition to laboratory experiments using synthetic ice panels. Details of these tests can be found in [10] including successful traversals up snowy slopes up to 35 degrees (Figure 2, middle). The second prototype, *EELS 1.5*, was designed for *vertical mobility* tests and demonstrated preliminary vertical mobility between two manufactured water ice walls in a walk-in freezer at the JPL ICELAB (Pasadena, CA). While these initial results were promising, a

Figure 2; Surface mobility tests of the EELS 1.0 prototype robot an ice rink *(top)*, on loose snow *(middle)*, and on loose sand *(bottom)*. Credit: NASA JPL

field test in a dynamic analogous environment to icy moons with naturally occurring features and challenges, and uncontrolled stimuli for the robotic systems to encounter and respond to are critical for maturing the technology, elevating the technology readiness level (TRL), and collecting engineering data to aid in further development of the project. To that end, this paper presents on results from the 2023 Athabasca field test we performed at in Alberta, Canada as detailed in section 2.
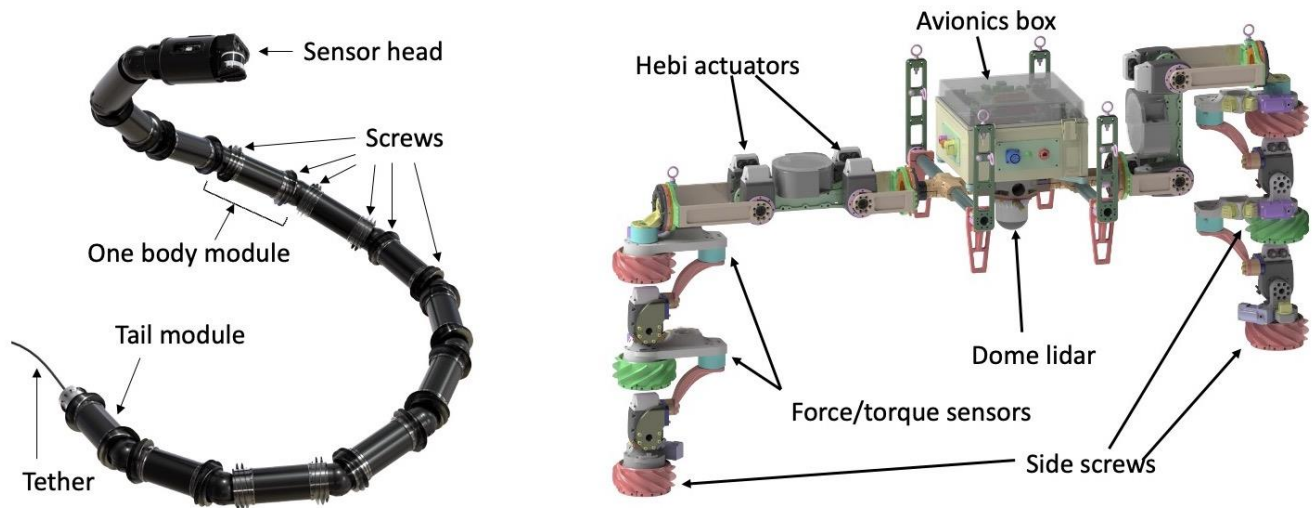
Figure 3: The EELS robot prototypes used for the field test. *Left*: The EELS 1.0 robot used for surface mobility testing in the field consists of 10 identical modules allowing the robot to change its 3D shape and propel itself across the icy undulating surfaces using its screws. A sensor head containing a 3D LiDAR, stereo cameras and an IMU enable autonomous waypoint navigation. *Right*: The EELS 1.5 robot used for vertical mobility testing in the field consists of two climbing arms attached to an avionics box. Each climbing arm contains shape actuators to expand width and conform to undulating terrain, screw actuators to climb, and heating elements to hasten the penetration of screws into the ice.

EELS 1.0 Hardware Overview

The EELS 1.0 hardware is designed for versatility. Its high-Degree of Freedom (DoF) mechanical configuration, as well as the unique *active-skin propulsion* mechanism [13], which propels the robot using the counter-rotating screws on the robot's "skin," allows a wide range of mobility modes. The mechanical system of EELS consists of body modules, a sensor head, and a tail module, as shown in Figure 3, More details can be found in [11, 15].

Body Modules – The backbone of an EELS robot is a linked chain of multiple identical body modules. Each adjacent body modules are connected by a joint with two DoF: twist (rotation around the body axis) and bend (rotation around an axis perpendicular to the body axis). Each body module can support two surface-mounted counter-rotating screws for active skin propulsion. The screws are rotating blades – they create strong traction on ice by penetrating into it while producing a thrust through rotation. A module's two screws have opposing threads, one is left-handed, and one is right-handed. By counter-rotating the screws, axial thrust is produced. By rotating the screws in the same direction, lateral force is produced. This unique screw propulsion provides extra degrees of freedom that allows a greater variety of mobility modes than that of biological snakes. The two screws on an EELS 1.0 module are driven by a single actuator and geared to always counter-rotate [13], while those on the future EELS 2.0 modules will be driven by two independent actuators. Hence, one EELS 1.0 module has three actuators (bend, twist, and screw) while one EELS 2.0 module will have four actuators. During surface mobility tests of EELS 1.0 prior to the field test at Athabasca Glacier, we found that the coupling of the two screws of each module is limiting because it precludes lateral motion. Therefore, in the field test, we removed one of the screws from each module, and reconfigured screws such that the handedness flipped from left-hand to right-hand between neighboring modules. (See Figure 3, left). Since EELS 1.0 has ten body modules, it has a total of 30 DoFs.

Sensor Head – The sensor head of EELS 1.0 has a scanning LiDAR, four pairs of stereo cameras (one pair on the front, one pair on the top, and two pairs on the side), an inertial measurement unit (IMU), and an NVIDIA's Jetson Xavier computing board for vision processing.

Tail Module – The tail module serves as the attaching point of the tether that supplies power and communication for the robot. It also accommodates another IMU. In the future, the tail module would accommodate the tether management system. Physical tether management would include bend and twist prevention as the robotic system descends into terrain features.

EELS 1.5 "Hebi" robot – The EELS 1.5 robot (Figure 3, right) has a substantially different configuration from EELS 1.0 that is worth an additional note. Since it is highly specialized for vertical mobility tests, some of the middle body modules are omitted and replaced with a simple avionics box. It has three body modules on each side, giving them the appearance of two "arms" attached to the avionics

3

box. The tether and a dome LiDAR are attached to the avionics box; hence it replaces the sensor head and the tail module of EELS 1.0. Each arm is capable of gradually increasing in width to push against ice walls. Shape actuators on the arm provide active compliance on the undulating ice walls. Each arm consists of three screws with one in counter rotation to the others. Screws are actively heated to increase the speed of penetration (via melting) into the ice.

EELS Software overview: NEO Autonomy
In our previous work [10], we introduced NEO a novel autonomy framework for controlling versatile high-degree-of-freedom robots such as EELS, aimed at exploring unknown and extreme environments like the geysers of Enceladus or the subsurface oceans of icy worlds. Distinct from conventional Mars mission strategies, NEO embodies resilience, adaptivity, and risk awareness. NEO supports fault-aware perception using both exteroception and proprioception, inspired by Erik Weihenmayer, the first blind climber to ever ascend the nose of El Capitan in Yosemite National Park, CA, USA using tactile inputs [12]. NEO tightly couples planning, perception, and control using machine-learning-based adaptation. Moreover, NEO incorporates risk-aware decision-making with integrated task and motion planning under consideration of uncertainty, enabling autonomous adaptation of actions to mitigate risks and maximize mission success. This paper presents experimental results showcasing these capabilities and discusses the potential for NEO in spearheading a new paradigm in space exploration.

EELS Instrumentation Overview

Miniaturized Capillary Electrophoresis – The instrument, designed for a single EELS module, employs capillary electrophoresis with capacitively coupled contactless conductivity detection (CE-C^{4}D) to analyze cations and anions in liquid water samples. A schematic is provided in Figure 4. Equipped with two C^{4}D detectors, it simultaneously analyzes both negatively and positively charged species. This cylinder-shaped instrument, with a 10 cm diameter and 32 cm length, is a modification of a prior underwater CE design [4]. The CE-C^{4}D is encased in a watertight housing with five ports: (1) sampling, (2) internal standard, (3) background electrolyte (BGE) supply, (4) waste removal, and (5) auxiliary. Two gravity-independent high-voltage reservoirs ensure its operation in any position or during motion [5].

In its tested configuration, the instrument accommodates 25 mL of BGE, 25 mL of water for rinsing, and 50 mL for waste. Additionally, it features a pneumatics and liquid processing module for solution delivery, dilution, spiking, and fluidic line pressurization and purging. All requisite liquids are delivered to the CE module, which houses separation capillaries, detectors, a high-voltage power supply, and an injection valve. This module executes the analytical process, encompassing sample separation and compound detection.
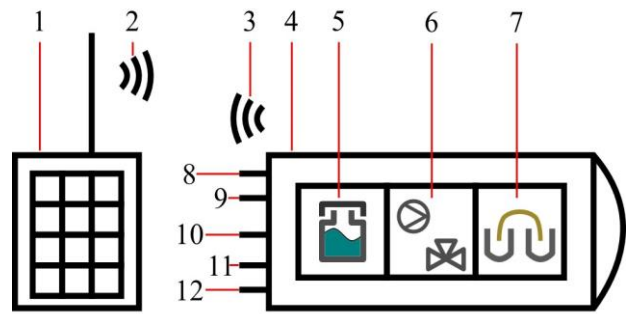
Figure 4: Diagram of the CE-C4D instrument. Annotations: 1 – Remote control, 2 – Command transmission, 3 – Status transmission, 4 – Instrument enclosure, 5 – Reagent and waste storage, 6 – Pneumatic and fluidic module, 7 – CE module, 8 – Sampling port, 9 - Internal standard port, 10 – BGE port, 11 – Waste port, 12 – Auxiliary port

Control and monitoring are achieved via a purpose-built low power remote using 900 MHz LORA for communication. The CE device is powered by a 4S1P Li-ion battery pack, sufficient to operate for a full day, with regulated voltages of 12, 5, 3.3, and -5 V for different modules. Custom firmware drives an automation engine. Moreover, the instrument can execute scripted protocols (e.g., priming, sampling, spiking) from an on-board SD card, where it also stores data.

Cryoegg Instrument (future) – The Cryoegg is a wireless sensor package designed to explore subglacial systems [6-8]. Its spherical form means that it can fit inside one of the EELS modules between screws (see Fig. 3) to allow autonomous release in a desired englacial or subglacial location. A future earth-science mission concept is for EELS to deploy a Cryoegg into a sub-surface channel to record temperature, pressure, and electrical conductivity of subglacial water over extended (seasonal to annual) timescales. Data are returned from the egg to the surface via radio and recorded by a satellite-linked, solar-powered transceiver. Work is currently underway to design a module that can integrate and release a Cryoegg in an englacial conduit. This terrestrial mission would demonstrate a future capability of delivering and deploying an instrument package into an otherwise inaccessible environment.

2. ATHABASCA FIELD TEST OVERVIEW
The field test took place on the Athabasca Glacier in Alberta, Canada, from September 12, 2023, to September 30, 2023. We conducted a prior, smaller-scale field test in the same site in September 2022, in which we tested two components of the EELS robot: the sensor head and the screws. The 2023 field test demonstrates the mobility subsystem in a future mission using two robots (EELS 1.0 and EELS 1.5), as well as component-level tests of science instrument and screws.

Demonstration in terrestrial analogues is a critical step for elevating the technology readiness level (TRL) of innovative technologies like EELS. The top-level goal of this field test was overall EELS technology maturation, which was broken into the below four objectives.

1. Demonstrate horizontal mobility on icy surfaces using the EELS 1.0 robot in a natural analogue environment.

2. Demonstrate vertical mobility (position hold and descent) in englacial conduits using the EELS 1.5 robot in a natural analogue environment.

3. Validate the operation of scientific instruments designed for future use in the EELS robot and collect measurements of glacial water chemistry and conduit geometries.

4. Characterize the mechanical interaction with side screws and natural ice through controlled experiments.

These objectives mapped to four types of tests we performed on the glacier, detailed in the next section.

Test Site Overview
The Athabasca Glacier, located in the Canadian Rockies, is a valley glacier that transports snow and ice from the Columbia Icefield to lower elevations. We chose Athabasca Glacier as our test site for multiple reasons. First, the glacier possesses a rich set of vertical features, such as moulins, ice channels, and crevasses [9]. The second reason for selecting Athabasca is the ease of access on account of nearby transportation and lodging. Suitable test sites are found within a 0.5 km^2 region of the glacier and within 250 m of the area accessed by tourist vehicles. The third reason is the highly supportive Canadian National Park service and the local communities. Since moulins and channels change in location, shape, and size over the timescale of days to months, we needed to scout the glacier and identify suitable test sites prior to the field test campaign. Our scouting team identified 22 moulins, two deep (>2 m) active channels (with water flow), and five deep (>2 m) dry/damp channels (little to no water flow), designated M1-22, AC1-2, and DC1-5, respectively. Our Base Camp was set up at a safe area near the most promising test sites. The following features were used in our tests, see Figure 5 for their locations.

BC1: This site is located within the Base Camp area at the north-east corner. The terrain is relatively flat with a downward slope towards north-east.
BC2: This site is also with the Base Camp area at the south-west corner. The terrain is richer in topography than BC1.
DC5: This channel was about 1 m wide and 3 m deep and had numerous sharp turns. The science team performed 3D mapping of approximately 80% of this feature.
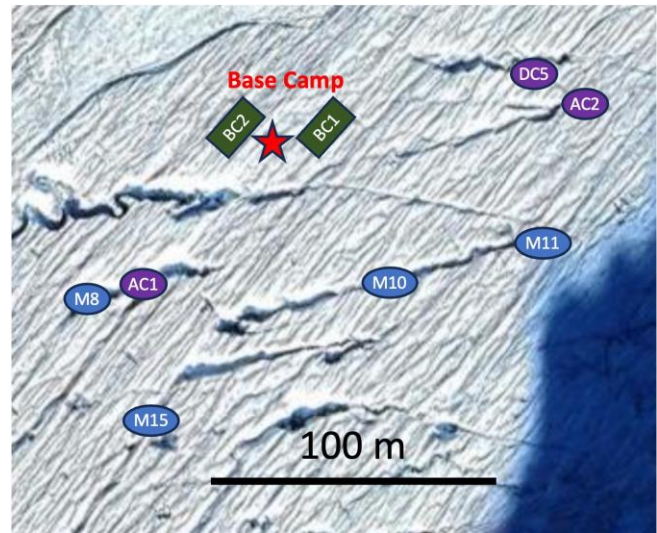
Figure 5 Map of the test site on Athabasca Glacier and the glacial features used for the tests. The positions of the features are approximate and the registration with the base map might not be perfect due to the glacial movement. The latitude and the longitude of the Base Camp was (52.198589, -117.244562).

M8: This moulin is a part of the AC1 active channel. It measures about 1 m in width and 8 m in depth, with a dry flat surface at the bottom suitable for humans to stand on, which made this site particularly appealing. The cross section has an irregular shape, and the wall has ripple patterns called *scallops*. This site was used for the first vertical mobility test.
M10: This moulin had an irregular cross section with smooth surfaces of 1.5 m – 2.0 m, narrowing towards the bottom at 10 m depth. It was used for the third and the last vertical mobility test.
M11: This moulin has near-cylindrical cross section with relatively smooth surface, mostly devoid of scallops. It has an unknown depth (at least 15 m) and 1.5 m width near the surface, which gets narrower at the deeper part. The top part of the moulin is connected to another shallower (~5 m deep) moulin with dry bottom, which served as a convenient "observation gallery." This site was used for the second vertical mobility test, and a nearby supraglacial pond was used for submerged operations of the CE instrument.
M15: This was the deepest moulin of those explored with an initial opening 22 m deep adjoining a long horizontal channel, followed by two additional 5 m drops and an ongoing subglacial channel, reaching at least 40 m vertical depth.
AC1: This channel was about 1 m wide and 2 m deep and had numerous sharp turns. The science team performed 3D mapping of approximately 80% of this feature.
AC2: This channel was 0.6-0.7 m wide and 2 m deep. The CE instrument was operated with autosampling in this channel.

Athabasca Glacier as an Ocean-World Analogue

While there is no perfect simulant on Earth to the icy surfaces of Enceladus and Europa, we posit that terrestrial glaciers with englacial conduits are sufficient analogues for initial mobility tests of the EELS robotic systems. Clustered glacial features including moulins, ridges, crevasses, and the ease of accessibility to these features, as well as proximity to logistical resources make the Athabasca Glacier a key analogue site. The chemical composition of the glacial ice at the Athabasca glacier is not an exact match for that of the Enceladus and Europa surface, however the expected temperatures of the ice walls in the warmer vent, i.e. Tiger Stripes of Enceladus, is expected to be near 0 C [1], and is a direct thermal analogue to the temperatures of the ice on Athabasca Glacier in September (-10 C to 0 C). As the main objective of this field test was to demonstrate vertical mobility against Earth gravity in englacial conduits at the Athabasca glacier, we assert that the robot resisting the forces of gravity while holding position or climbing up and down in an englacial conduit is analogous to an Enceladus vent exploration robot descending while resisting the upwards forces of an active plume. Active heating of the screws is also crucial to maintain penetration into the ice while climbing.

Environmental Sampling at Athabasca

Environmental data was collected at the Athabasca Glacier in the following formats:

i) Glacial water samples for in-situ inorganic ionic analysis via Capillary Electrophoresis (and for storage for future in-laboratory testing), collected at the following EELS 1.5 robotic test sites; Generator Stream, Active Channel 2, Pool Near M11, 4th Ravine, 4th Ravine (Sediment Rocks), 7th Ravine, M8.

ii) 3D Topographical point cloud maps from the traverse paths of the EELS 1.0 sensor head at Active Channel 2 and Base Camp (as well as prior data from Athabasca 2022 field campaign that illustrate clustered englacial features in detail

iii) Weather metadata from the Athabasca Glacier was collected from an on-site weather station and online services including temperature, precipitation, humidity, wind speed.

iv) cone penetrometer data from horizontal and vertical ice-surfaces at various depths and porosities collected at the Mobile Screw Testbed test sites.

The above data will inform the physical properties and environmental conditions needed to recreate simulated ice for future robotic system testing and characterization in a walk-in freezer or laboratory environment.

Field Test Logistics

The field test spanned over 20 days and involved two robots, one mobile testbed, significant test, and support equipment, and over 40 engineers, scientists, safety and supporting staff. As a result, the field logistics were highly complicated and required careful planning. We set up the *base camp* on the glacier near the test sites. The robots and equipment were shipped from JPL to a nearby facility by truck, transported to the base camp by helicopter, and stored in the base camp over the entire duration of the field test. On every test day, personnel arrived at the glacier by a snow coach and then walked to the base camp. One or more test sites were selected depending on the test objective(s) of that day. Robots and gear were transported from the base camp to the operation station on sleds or hand carried. The *operation station* was set up at the site, as shown in Figure 6 (following page). At the end of each test day, the operation station was disassembled and the robots/gear were packed up and transported back to base camp for overnight storage. At the end of the field campaign, the robots and gear were transported back to a nearby facility by helicopter, and then returned to JPL by truck.

Field Safety

The existence of challenging glacial terrain features such as moulins, crevasses, and vertical conduits are ideal testing grounds for robots, but pose significant and deleterious risk to staff if not traversed with utmost safety and respect. Multiple injuries and fatalities are recorded on glaciers annually [14], even by the most experienced mountaineers. The risk is amplified in our case because tests were performed within vertical glacial features. All JPL personnel underwent training in glacier travel, hazards, and vertical rappelling/ascending. This training and preparation provided by Direct Action Vertical (DAV), subject matter experts in vertical, tactical, and rescue operations. DAV provided expedition coordination, rigging operations, and maintained a 1:2 ratio to science/engineering personnel throughout the field campaign.

Test schedule overview

The entire field test campaign spanned 20 days starting on September 11, 2023. Table 1 shows a high-level summary of day-to-day activities. The scale and complexity of the test campaign required substantial logistical burden. The team planned the logistics carefully and there was no major deviation from the plan in terms of logistics. Still, it took 8 days out of the 20-day expedition for personnel/equipment transportation, which underscores the logistical complexity that we were faced with. We would like to highlight the fact that the technical success of the field test, which will be detailed in the next chapter, was a product of the extensive effort the team spent for the planning, management, and execution of logistics.
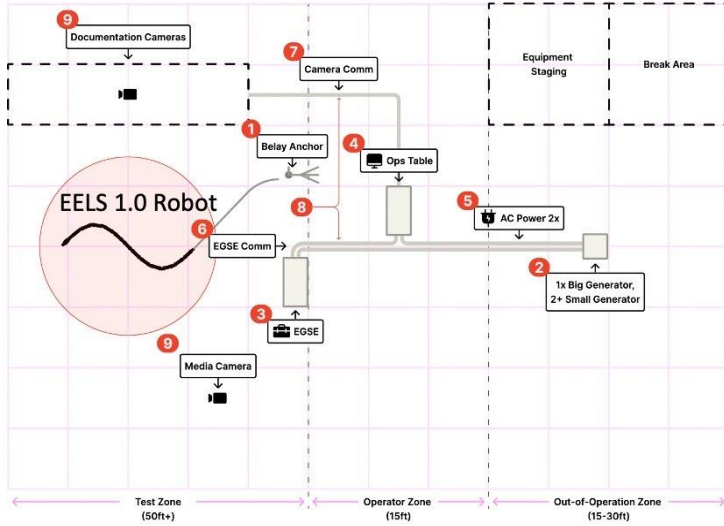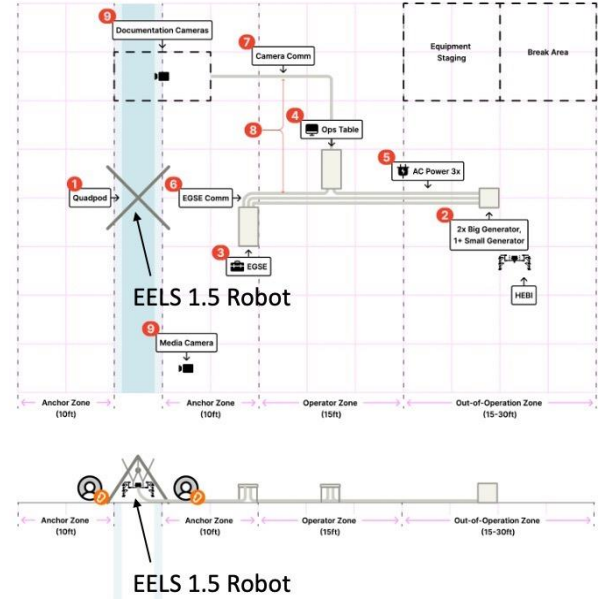
Figure 6: The test set-up diagrams. *Left* Surface - (1) Belay anchor, (2) generators, (3) electrical ground support equipment (EGSE), (4) operation tables, (5) AC power lines, (6) EGSE communication lines, (7) camera communication line, (8) cable protection, (9) context and media cameras. *Right* Vertical - (1) Quadpod and anchors, (2) generators, (3) electrical ground support equipment (EGSE), (4) operation tables, (5) AC power lines, (6) EGSE communication lines, (7) camera communication line, (8) cable protection, (9) context and media cameras.

Table 1: Summary of day-by-day activities during the field test. The four main activities are labeled as "Surface" (surface mobility tests with the EELS 1.0 robot), "Vertical" (vertical mobility tests with the EELS 1.5 robot), "Science" (science instrument tests), and "Screw" (screw-ice interaction experiments). Note that a substantial amount of time and effort was required for staff/equipment transportation and test set-up and wrap-up activities due to the scale and complexity of the field test. Day 1 was Sep 11, 2023. Out of the 20 days, we had 9 full-days and 2 half-days for test activities. 8 days were needed for logistics and 1 day was lost due to unfavorable weather.

Day	Activities
1	Advanced team left JPL and arrived in Calgary. The shipment truck arrived in Athabasca.
2	The advanced team arrived in Athabasca and started unloading, while the 15-person main team left JPL and arrived in Calgary.
3	The advanced team conducted initial scouting of the glacier to identify suitable test sites. The main team and the safety guides arrived in Athabasca.
4	Robots and gear were transported to the Base Camp on the glacier by a helicopter and Base Camp was established.
5	**Vertical**: Test rig was set up over the "M8" moulin while the shake-out test at the Base Camp of the EELS 1.5 robot was conducted on site. **Science**: LiDAR scan of M8 was performed. **Screw:** Conducted first screw mobility tests.
6	**Vertical**: Dress rehearsal of vertical position hold test was performed in M8. **Science**: The DC5 dry channel was mapped with LiDAR. **Screw**: Three different screws were tested on ice at the Base Camp.
7	**Surface**: Shake-out test of EELS 1.0 and open-loop surface mobility test in BC1. **Vertical**: Successful vertical position hold was achieved in M8. **Science**: The M8 moulin was re-mapped with LiDAR, and preliminary scans were collected of M11. Conductivity measurements were performed with a handheld probe at DC5 and M8, as well as various supraglacial streams, to identify suitable test sites for the CE instrument. **Screw**: Surface screw tests were performed at the Base Camp.
8	Unfavorable weather. A small group conducted scouting and Base Camp maintenance activities.
9	**Surface**: Demonstrations of screw- and shape-based gaits at BC1 were performed. **Vertical**: Test rig was set up over the "M11" moulin. **Science:** Performed LiDAR mapping of AC1 and inspected M15. **Screw:** Additional screw tests were performed at the Base Camp.
10	**Surface:** The sensor head was attached to EELS 1.0; the team successfully completed the check-out of the sensor head. **Science**: Initial check-out of the CE instrument was conducted.
11	**Vertical:** EELS 1.5 successfully held the vertical position using force feedback control and climbed up the M11 moulin a few cm. **Science**: 3D scans were taken in M15 with Scaniverse; water samples were collected at a supraglacial stream and analyzed with the CE instrument on the ice at Base Camp.
12	**Vertical:** EELS 1.5 successfully held the vertical position using force feedback control and climbed up the M11 moulin a few cm. **Science**: Performed a spiked blank measurement with the CE instrument; mapped more of M15 using Scaniverse.
13	The team scouted moulins to identify the next site for vertical tests. Activities interrupted due to heavy rain.
14	**Surface**: EELS 1.0 was tested in AC2; it crawled into and out of the channel by itself. **Vertical**: Test rig was set up at M10. EELS 1.5 was winched down into the moulin and tried position hold with force control but did not succeed. **Science**: The CE instrument was placed in a water stream at the bottom of AC2 and successfully sampled the water and performed an analysis in situ. **Screw**: The screw testbed was placed vertically on the ice wall of M8 and tested the new screw with a 10 degree pitch angle.
15	**Surface:** EELS 1.0 obstacle avoidance tests were performed at BC2 with the sensor head. **Vertical**: The EELS 1.5 robot made a controlled descent in the M10 moulin over ~1.5 m using a shape-based control. **Science:** The CE instrument was submerged in a pool of glacier water near M11 and successfully performed in-situ analysis.
16	**Surface:** EELS 1.0 obstacle avoidance tests were performed at BC2 with the sensor head. **Vertical**: The EELS 1.5 robot made a controlled descent in the M10 moulin over ~1.5 m using a force feedback control. **Science**: The CE instrument was deployed in both the 4th and 7th active surface channels west of base camp and performed successful sampling and sample conductivity measurements.
17	**Science**: CE was deployed deep in M8 moulin and performed successful sampling and conductivity measurements. The base camp was demobilized. Robots and gear were transported to a nearby parking lot by a helicopter.
18	Robots and gear were loaded on the truck.
19	Additional shipping logistics were handled. The team moved to Calgary.
20	The team left Calgary.

3. SURFACE MOBILITY TEST RESULTS

The surface mobility tests demonstrated the EELS 1.0 robots ability to navigate sloped and undulating glacial terrain using the following gaits: i) fixed-shape gaits, where the robot's shape is locked and it moves across the surface with its screws, ii) sidewinding, where the robot moves laterally using only its shape actuators, iii) open-loop leader follower, where the robot follows a trajectory using its screws to propel forwards, and iv) closed-loop leader follower, the same as iii) but using exteroceptive feedback from the head to plan paths and correct for drift. Details on these algorithms can be found in [10]. Five surface mobility experiments were performed at three sites with various hardware and software configurations, as summarized in Table 2. The EELS 1.0 robot was used for all tests. Two types of screws were tested: metal screws with a 30 degree pitch angle and plastic screws with a 15 deg degree pitch angle. The results from the first two tests on Days 7 and 9 demonstrated better mobility with the plastic screws. Therefore, we used the plastic screws for the remaining tests. The first two experiments tested open-loop mobility (i.e., without mapping and localization) without the sensor head, while the last three tested closed-loop mobility with the sensor head. These experiments demonstrated EELS' capability to autonomously navigate and traverse glacial surfaces with steep slopes and deep undulations.

Table 2: List of surface mobility tests.

Day	Screw	Sensor head	Test site
7	Metal	No	BC1
9	Plastic	No	BC1
14	Plastic	Yes	AC2
15	Plastic	Yes	BC2
16	Plastic	Yes	BC2

Surface Test 1 (Day 7) – Robot check-out activities were performed, followed by simple mobility tests. The EELS 1.0 robot equipped with the metal screws was manually commanded to perform fixed-shape gait motion in x (forward), y (sideways), and yaw (rotation about z) with constant bend angles. The robot initially took the "pencil" configuration (i.e., all joints are straight), then the "banana" configuration (i.e., a uniform, relatively small angle at every bend joint such that the robot takes a banana-like shape). The first few cm of the glacier surface consisted of unconsolidated materials (snow, broken ice) that caused the metal blades to chew the terrain without providing thrust, belly panning the robot.

Surface Test 2 (Day 9) – The larger, deeper, plastic screws were put on the robot and the same tests were repeated at the

Figure 7: EELS 1.0 descending into the AC2 channel in Surface Test 3 on Day 14

same site as Surface Test 1. In the pencil configuration, the robot could reliably drive forwards and backwards but did not have any control authority in sideways motion or turning. Control authority was restored when the robot was in the banana configuration, with all bend actuators set to 0.1 rad angle or higher. This lack of control authority when the robot was straight is likely due to the low pitch angle of the screws and lack of sufficient penetration with plastic screws into the ice. The plastic screws worked better on unconsolidated materials due to its deeper threads compared to the metal screws. Following this success, the team moved on to test the "leader-follower" gait, in which the operator commands a waypoint, a path planner in NEO plans a path from the robot position to the waypoint, and each module follows the path of the preceding modules like a train. The team also tested upslope mobility with the leader-follower and the side-winding gaits but did not yield promising results. The side-winding gait, which moves in the y (side) direction, slipped on slope likely because of the small pitch angle (15 degrees) of the plastic screw.

Figure 8: EELS 1.0 avoided a negative obstacle semi-autonomously in Surface Test 4 on Day 15.
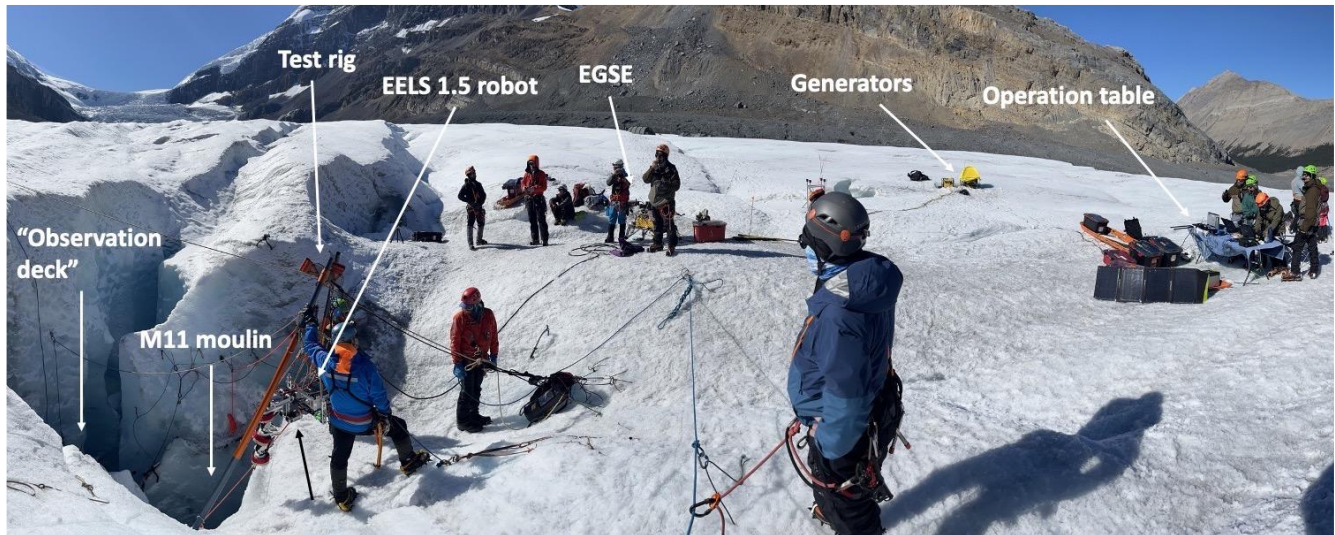
Figure 9: Vertical mobility test at the M11 moulin on Day 12

Surface Test 3 (Day 14) – The sensor head was attached to the EELS 1.0 robot prior to the test. The robot was placed at the mouth of AC2 and was commanded to enter the channel with autonomous path planning using the leader-follower gait. It used the LiDAR on the sensor head to scan the environment and localize itself, then plan a path that minimizes traverse distance while avoiding excessive slopes and hazards. The robot successfully descended the slope ~10 m and reached the bottom of AC2 (Figure 7). The team commanded the robot to move backward and climb the slope to exit AC2. Operators had to actively manage the tether during this test case. This motion turned out to be more challenging because the tail section, which was now leading the robot, constantly got stuck. As a result, the team manually commanded the tail to raise or lower to comply with the terrain while manually commanding the robot's path. The robot successfully climbed the slope.

Surface Test 4 (Day 15) – The focus of this day's test was to test obstacle avoidance features. The test took place at BC2. The robot was commanded to avoid a negative obstacle (the pool shown in Figure 8) using the leader-follower gait. It raised its head, scanned the environment, successfully recognized steep slopes around the negative obstacle, and stopped itself.

Since the leader-follower gait does not support backward driving and the plastic screws place mechanical limits on minimum bend angles, the robot could not find a feasible path to proceed. After manual interventions, it successfully found a feasible path, navigated around the obstacle, and made 10-15 m progress. There was substantial rainfall in the preceding days, which removed most of the unconsolidated materials and exposed the ice. This could be the reason for why the plastic screws experienced less traction than in Surface Test 2, which limited the control authority of the robot. The team decided to proceed with the plastic screws due to the time required for changing the screws. Additionally, the robot experienced issues with its IMU.

Surface Test 5 (Day 16) – The tests on this day were similar to the prior day. It was commanded to avoid the same negative obstacle and resulted in the qualitatively same result.

Lessons Learned – The series of tests demonstrated the EELS 1.0 robot's ability to move across icy surfaces with undulations and slopes, as well as the basic components of autonomous mobility including path tracking, mapping, localization, and path planning. Screw design is crucial for controllable mobility across natural icy surfaces. The short, 30 deg metal screws that worked well on the ice rink [10], high-centered the robot on the porous glacier ice. The longer 15 deg plastic screws provided better traction but failed to resist lateral slip and had little to no control authority to move laterally. The surface mobility tests, as well as the screw mobility tests described later, have provided valuable data for optimizing the screw design. Screw traction can also be improved by enhancing the body compliance to the terrain through software such that most of the screws are in contact with the surface. This is a requirement for moving across undulating and sloped terrain. A final observation was that hardware that worked well in a laboratory setting can often break down in the field due to cold temperatures and high humidity (snow, rain). Overall, the tests made a compelling demonstration of the surface mobility of EELS and gave us clear understanding about what to improve. The data collected from the experiments are still under analysis. More detailed results will be reported in later publications.

3. VERTICAL MOBILITY TEST RESULTS

We conducted seven vertical mobility tests at three sites, as summarized in Table 3. The test procedure was highly complicated due to the need of placing a ~50 kg robot in a vertical hole, which poses substantial danger to the personnel. Figure 9 shows the test set-up on Day 12, which provides a glimpse of the complexity of the test. There was substantial trial-and-error to figure out a safe and reliable process. The test preparation took at least two to three hours, and the close-out activities also took one to two hours every day, which

10

limited the time we could use for experiments. Nonetheless, we demonstrated both vertical position hold and controlled vertical motion while supporting the full weight of the robot against gravity. We furthermore demonstrated autonomous vertical controls with little reliance on the operator to descend. These are key mobility requirements for future vent exploration robots.

The focus of the test was two low-level control functions: i) vertical position hold and ii) quasi-static vertical motion. Vertical position hold means the robot pushes the two opposing walls strong enough to support its own weight, like a rock climber's chimney move. The test process goes as follows:

1. The robot was lowered by rope and coarsely positioned via taglines.
2. Robot Wranglers on rappel in the moulin finely positioned the robot.
3. Robot Operators commanded the arms to expand and make contact with the ice walls.
4. The rope was slackened to verify that the robot supported its own weight.

If the robot did not shift or fall, vertical position hold was achieved. Closed-loop temperature control was performed on the screws using active heating to let the screw blades penetrate deeper into ice. Vertical motion was commanded by rotating the screws using a closed-loop controller while both roll and pitch were controlled to zero and the arms were controlled to maintain contact on uneven walls. Two controllers were used for making and maintaining contact between the screws and the walls. The first is shape-based control, which brings each screw to operator-specified
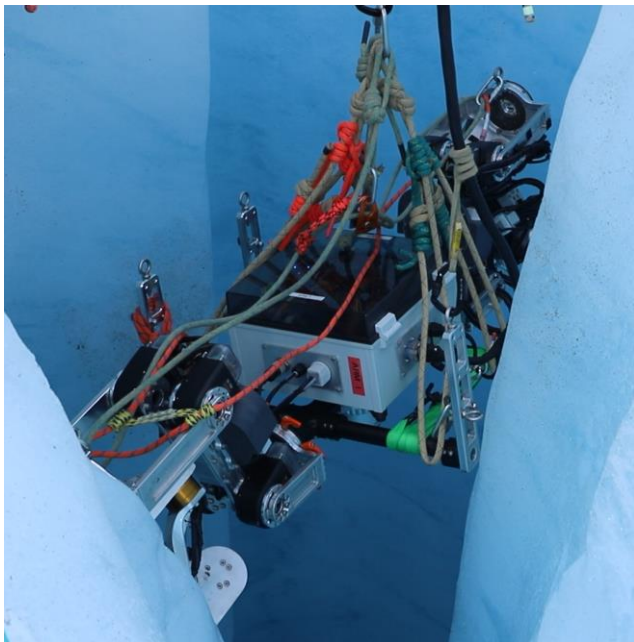
positions. This controller is simpler but requires the operators to manually adjust the set points through visual confirmation. It also cannot adapt to changing geometry when the robot moves or when screws significantly melt into the ice. The second approach is called simultaneous shape, contact, and force (SCF) control. The SCF controller pushes out the arms until a specified normal force at each of the six screws is achieved. It does not require manual configurations of setpoints at every run and it can adapt to varying geometry during the motion. However, the estimation of the contact force has uncertainty, and since the desired force at six contact points is achieved via the control of eight joint torques, it is an under-constrained problem. The details of the technical solutions will be presented in a separate publication. Here, we will present the outcomes of the experiments.

Vertical Test 1 (Day 6) – The team selected M8 as the first test site mainly due to its proximity to the Base Camp. Also, because M8 is relatively shallower than other moulins, it was deemed to be safer. The EELS 1.5 robot suffered electrical issues due to snow entering the connectors during transport and the test was turned to a dress rehearsal of physical operation with the onboard computer powered off.

Vertical Test 2 (Day 7) – The team performed a single run of robot operation in the moulin and achieved vertical position hold for the first time using the shape-based control, which lasted for ~5 minutes until the robot lost power due to an electrical issue. No attempt of vertical motion was made. The team decided to end the experiments at M8 because lowering the robot into this moulin turned out to be challenging due to range-of-motion limitations of EELS 1.5 hardware which will be addressed in a future version of the robot, EELS 2.0. Furthermore, the walls of this moulin were

Figure 10: EELS 1.5 during the successful vertical descent in M10 during Vertical Test 7 on Day 16. Note the slack rope, indicating the robot is holding its own weight.
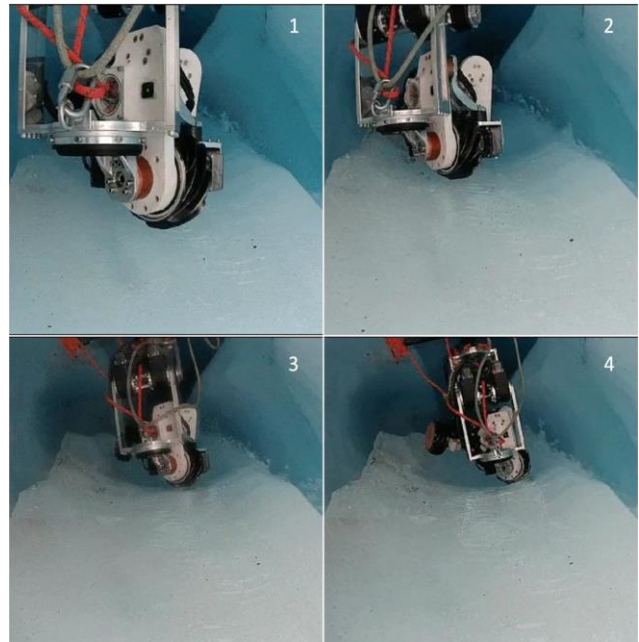
Figure 11: The motion of one of the arms of EELS 1.5 during the successful ~1.5 m vertical descent in Vertical Test 7 on Day 16.

11

highly undulated with many scallop features and was considered challenging for making significant vertical motion without a vertical motion planner, which is our future work.

Vertical Test 3 (Day 11) – We chose M11 as the new site for its favorable geometry for logistics and safety of rigging and lowering the robot. The walls were relatively smooth compared to M8. The robot successfully held its vertical position using SCF for the first time. We performed multiple tests, all of which used the SCF controller. We then commanded the robot to rotate the screws to climb. The robot climbed about 2 cm and slid down a few cm. The fall was arrested by the SCF controller reestablishing wall contact. The belay line did not take the weight of the robot.

Vertical Test 4 (Day 12) – We repeated the same experiments as in Day 11 with modifications to the SCF controller. It successfully held its vertical position again and climbed up ~5 cm until it slid down. One of the reasons the robot could not make substantial motion was the taper of the wall. As it climbed, the distance between the walls widened and the robot tended to lose contact. The SCF controller should have been able to adapt to it, but it needed additional tuning.

Vertical Test 5 (Day 14) – We set up the rigging at the M10 moulin, which was less tapered than M11. We had a short duration of time to perform experiments after setting up the rigging. A new version of SCF was deployed. The robot did not achieve vertical position hold nor motion on this day.

Vertical Test 6 (Day 15) – We conducted two tests this day. In the first test we used the improved SCF, but observed unstable oscillations. In the second test, the shape-based controller was used to bring the arms into contact and successfully held the vertical position. We then commanded the robot to rotate the screws and it successfully descended ~1.5 m vertically. Notably, the robot pitched off vertical, but it recovered by itself and continued the descent.

Vertical Test 7 (Day 16) – The oscillation issue in the SCF controller was fixed, and the team performed three runs. In the first run, the robot successfully contacted the walls and held its vertical position solely using SCF. However, the screw heaters did not turn on due to a generator fault. The robot was commanded to descend without the screw heaters but broke traction soon after. In the second run, the generator issue was fixed, and the robot successfully held its vertical position, but the experiment was terminated prematurely due to an operator error. In the third run, the robot successfully held the vertical position again, and was commanded to rotate the screws. It successfully descended the moulin by ~1.5 m fully autonomously.

Lessons Learned and Future Work – The robot robustly held its vertical position in three moulins, each with substantially different wall geometry. Vertical motion was less robust to unfavorable geometry. Nonetheless, achieving multiple ~1.5 m-controlled descents is a highly promising preliminary result. In the future, it will be made more robust by improving the estimation of the contact force and the force admittance control. Additionally, the robot's dome LiDAR was solely used for data collection. The LiDAR's point cloud was not used in the control loop. As a result, the robot did not use NEO's higher-level planning capabilities including motion planning and action planning. In future experiments, using perception in the loop with motion planning will enable the robot to handle more complex geometry by choosing the most promising robot configuration and screw placements for the planned motion. Risk-aware action planning would allow the robot to select a sequence of actions that would most likely achieve the prescribed goals. The data collected throughout the tests, including robot telemetry and 3D scans, will be highly valuable for improving the robot hardware, maturing the controllers, and developing higher-level autonomy capabilities.

4. SCIENCE INSTRUMENT EXPERIMENT RESULTS

The CE instrument underwent three testing phases: (a) Deployment on glacier ice with sampling from a 50 mL falcon tube, which served as the collection vessel; (b) partial submersion in a supraglacial stream for sample collection and analysis; and (c) full submersion in a supraglacial pool for sample collection and analysis (Figure 12). All tests were successful, yielding valid analytical results. Figure 13.A and B displays representative data such as instrument temperature and power consumption, Figure 13.C presents an electropherogram of an actual sample. The remote operation of the CE instrument from the basecamp eliminated the need to remain in potentially hazardous zones where the device was stationed. Notably, signal strength diminished when the instrument was deployed in channels, moulins, or fully submerged. However, despite this reduction, the signal remained sufficiently robust to ensure effective operation

Figure 12. In-situ analysis of a supraglacial pool near M11 with the submerged CE instrument.
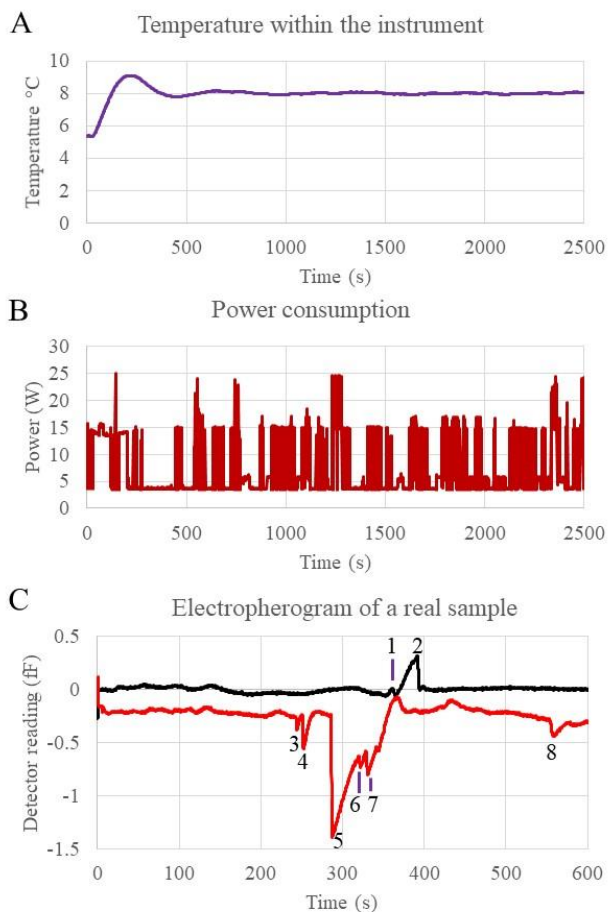
Figure 13. Collected data during analysis. (A) Temperature regulation profile during sampling and sample preparation. (B) Power consumption during sample and sample preparation. (C) Electropherogram of a real sample during separation. Peaks: 1 – SO42-, 2 – Cl-, 3 – Cs+, 4 – K+, 5 – Ca2+, 6 – Mg2+, 7 – Na+, 8 – unidentified

from the basecamp, which was always within 200 m of the test site.
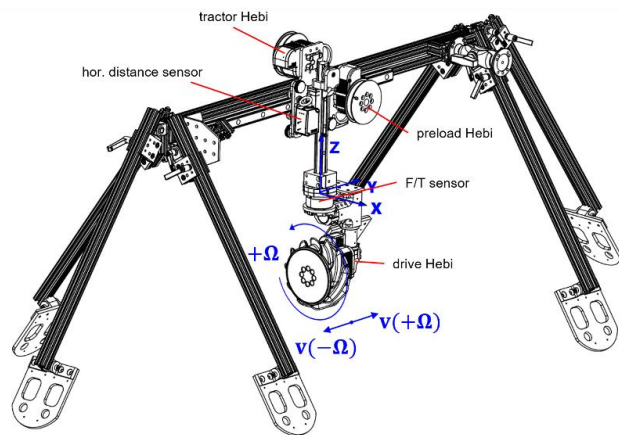
Figure 14. CAD model of the field deployable screw mobility testbed

The instrument demonstrated proficient temperature regulation. During the sampling protocol, power consumption peaked at 25 W, with a median consumption of 3.9 W and an average of 7.5 W. For the separation protocol, the peak power consumption was 16.2 W, with a median of 4.3 W and an average of 4.5 W. Following the analysis, the 0.55 μM Cs^+ peak was used as the internal standard. Additionally, we successfully quantified constituents such as K^+, Na^+, Mg^{2+}, Ca^{2+}, SO_4^{2-}, and Cl^- in the real samples. Detailed results will be discussed in future publications.

5. SCREW EXPERIMENT RESULTS

Figure 14 showcases the field-deployable screw mobility testbed designed to characterize in-situ screw performance. The testbed consists of an 80/20 frame and a detachable screw carriage containing sensors and electronics. The frame can be securely anchored via ice screws, adjusted for variations in terrain topography and roughness, and positioned in different configurations to investigate screw mobility performance on various terrains, including horizontal icy surfaces and vertical subsurfaces within the Athabasca glacier's moulins.

A rail system on the frame enables horizontal travel of the screw carriage while a secondary rail system on the screw carriage itself allows for vertical motion of the end effector where screws with different geometries can be attached. Figure 15 presents the different screws tested with the field deployable screw mobility testbed during the field test at the Athabasca glacier, showcasing differences in their length, pitch, thread depths, and materials.

An ATI Mini 58 Force/Torque (F/T) sensor is positioned directly above the screw to measure screw reaction forces and torques. The system is powered by three Hebi X8-16 series-elastic actuators that offer precise control and telemetry
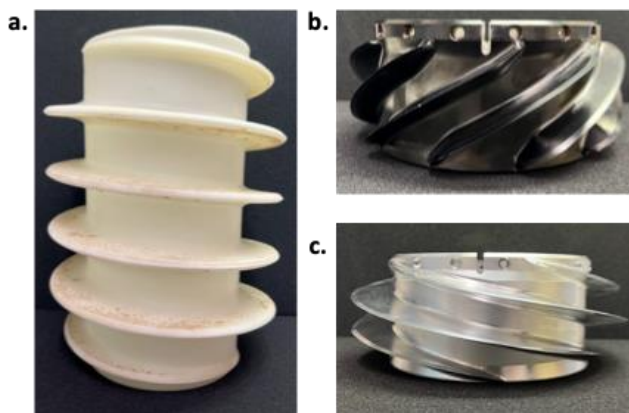
Figure 15. Images of three screws tested on the field deployable screw mobility testbed, where *a.* represents a 15 deg lead angle, 32 mm deep thread, 255 mm long screw 3D printed using Formlabs 4K resin; b. shows a 30 deg lead angle, 15 mm deep thread, 68 long Al 7075 black anodized screw; c. shows a 10 deg lead angle, 25 mm deep thread, 68 mm long Al 7075 (non-anodized) screw.

13

feedback. One actuator controls screw rotation (drive Hebi), while another actively controls preload via a cable-pulley system (preload Hebi). A third, dual-purpose actuator can provide forced horizontal motion of the screw carriage along the rail (i.e., shear) or introduce actively controlled traction loads (tractor Hebi). Laser distance sensors track the screw's horizontal and vertical position. A tether connects the carriage to an external electronic box, housing power supplies, data acquisition systems, and an emergency stop. Control is managed through a custom MATLAB GUI, logging relevant telemetry data at 15 Hz.

The field deployable screw mobility testbed supports a range of screw tests, namely surface penetration test, linear shear test, and traverse test. In the surface penetration test, a static screw with a given temperature is placed on the surface with a predetermined preload and the vertical position is tracked over time to measure the rate of penetration. In the shear test, a static screw is placed at one end of the horizontal rail system with a predetermined preload and orientation (e.g., threads parallel or perpendicular to the shear direction). The screw is then incrementally sheared using the tractor Hebi. The shear test yields different outputs depending on the screw's orientation, including friction coefficient, grip coefficient, and static traction. In the traverse test, the screw starts at one end of the horizontal rail system with a predetermined preload. The drive Hebi is assigned an angular velocity and rotation direction to move the screw carriage horizontally along the rail. This test measures slip factor, side force, and force direction.

Experiments using the field-deployable screw testbed were carried out primarily in two ice types in the Athabasca glacier: surface ice near the Base Camp (Figure 16), and "blue" ice on the walls of the M8 moulin (Figure 17) to emulate the terrains encountered by the EELS 1.0 and EELS 1.5 robots, respectively. Characteristics of the surface ice include a porous appearance from localized melting (and refreezing) due to sun exposure, where pore sizes of the top surface were as large as ice chunks. Ice chunks had structural integrity rather than exhibiting granular, non-cohesive

Figure 16. Field-deployable screw mobility testbed on a horizontal surface ice near the Base Camp.

Figure 17. Field deployable screw mobility testbed on a vertical wall (blue ice) in the M8 moulin

properties. Active melting occurred often at the surface, with air temperatures exceeding 5 C throughout most of testing and constant sun illumination from the sun. Surface ice was clearly weaker in bearing and shear strength when compared to blue ice. Blue ice could support at least 250 N/screw (with 100 N preload) during the upward traverse with certain screws. The surface ice would often fail without any traction load during traverse experiments. Results that quantitatively assess shear strength and traction load for the three screw geometries over the two ice types will be presented in future publications. However, a summary of high-level insights is given here. The 15 deg, 32 mm depth, 255 mm long screw performed significantly better than the other two screws in surface traverse conditions. The screw did not stall during traverse runs and was able to pull at least a 40 N traction load, whereas the other tested screws stalled often during the no-load traction traverse test. The 10 deg, 25 mm depth, 68 mm long screw performed best in blue ice, where small penetration amounts were able to lift at least 90 N of vertical load. Further, the thermal properties of screws were important factors when determining the rate and maximum depth of penetration into ice, with aluminum 7075 screws sinking significantly deeper than the screw made of 4K resin from Formlabs. Penetration depth is strongly correlated to how much traction a screw can support in a terrain type.

6. CONCLUSION

The 20-day field test campaign on Athabasca Glacier successfully demonstrated surface mobility with the EELS 1.0 robot and vertical mobility with the EELS 1.5 robot. Additionally, in-situ sampling and CE measurements were conducted with an instrument sized for an EELS body segment. We also conducted a series of terramechanics experiments to characterize the screw-ice interaction and inform future screw designs. The mobility tests demonstrated the basic horizontal and vertical mobility of EELS on a terrestrial analogue to icy moons. Surface mobility trials validated the EELS 1.0 robot's ability to move across icy undulating terrain while exposing some key lessons learned for future development improvements. Vertical mobility trails showed our robot's ability to perform both vertical position holds and stable autonomous vertical motion in englacial conduits. These mobility capabilities are required for future vent exploration robots that need to traverse harsh surface terrains to access vent openings. Then descend the vent while withstanding variable plume forces to access the liquid ocean. All through terrains that are uncharacterized prior to landing. The successful demonstration of the CE instrument suggests that EELS can perform astrobiologically relevant in-situ observations. The data acquired from the tests will inform future technology development applicable to icy and terrestrial moons.

7. ACKNOWLEDGEMENTS

8. REFERENCES

[1] Ono, Masahiro, et al. "Enceladus vent explorer concept." *Outer Solar System: Prospective Energy and Material Resources* (2018): 665-717.

[2] Chodas, Mark, et al. "Enceladus Vent Explorer Mission Architecture Trade Study." *2023 IEEE Aerospace Conference*. IEEE, 2023.

[3] Teolis, Ben D. et al. "Enceladus Plume Structure and Time Variability: Comparison of Cassini Observations. *Astrobiology* (2017): 926-940.

[4] Drevinskas, Tomas et al. "Submersible Capillary Electrophoresis Analyzer: A Proof-of-Concept Demonstration of an In Situ Instrument for Future Missions to Ocean Worlds." Analytical Chemistry. (2023): 10249–10256.

[5] Drevinskas, Tomas et al. "A gravity-independent single-phase electrode reservoir for capillary electrophoresis applications." (2023): 1047-1056.

[6] Bagshaw, Elizabeth et al. "Novel wireless sensors for in situ measurement of sub-ice hydrologic systems." *Annals of Glaciology* (2017): 41-50.

[7] Bagshaw, Elizabeth et al. "Prototype wireless sensors for monitoring subsurface processes in snow and firn." *Journal of Glaciology* (2018): 887-896.

[8] Prior-Jones, Michael et al. "Cryoegg: Development and field trials of a wireless subglacial probe for deep, fast-moving ice." *Journal of Glaciology* (2021): 627-640.

[9] Gulley, J., Benn, D., Müller, D., & Luckman, A. (2009). A cut-and-closure origin for englacial conduits in uncrevassed regions of polythermal glaciers. *Journal of Glaciology,* 55(189), 66-80.

[10] R. Thakker *et al.*, "EELS: Towards Autonomous Mobility in Extreme Terrain with a Versatile Snake Robot with Resilience to Exteroception Failures," *2023 IEEE/RSJ International Conference on Intelligent Robots and Systems (IROS)*, Detroit, MI, USA, 2023

[11] M. Gildner et al., "To Boldly Go Where No Robots Have Gone Before – Part 2: The Versatile Mobility of the EELS Robot for Robustly Exploring Unknown Environments", *AIAA Scitech 2021 Forum*. 2021.

[12] How Did a Blind Man Climb Yosemite's El Capitan in a Day? 2016. Adventure https://www.nationalgeographic.com/adventure/article/blind-climber-sets-el-capitan-record

[13] Georgiev, N. Efficiency Estimation and Optimization of Multistage Compound Planetary Gearboxes and Application to the Design of the Active Skin Propulsion of EELS. 2023 IEEE/RSJ (IROS), 4412-4419.

9. BIOGRAPHY

Michael Paton is a Research Technologist in the Robotic Mobility Group at JPL. He has worked on autonomous navigation for multiple extreme-terrain rovers. He lead the EELS Athabasca field test and co-lead the EELS autonomy efforts.

Richard Rieber is a systems engineer in the Robotic Ops and V&V group at JPL. He co-led the logistics planning of the Athabasca field test. He previously worked as the Mobility Flight Systems Engineer for the M2020 Perseverance rover, seeing the subsystem through design, fabrication, testing, and commissioning. He also worked testing and operations for the SMAP and Deep Impact missions.

Sarah Cruz is a mechanical engineer in the Planetary Sample Acquisition and Handling group at JPL. She served as the Icy Simulant & Testbed Facility Lead on EELS, facilitating and advising on robotic interactions with icy simulants in the JPL ICELAB and co-led logistics for the Athabasca 2023 field campaign.

Elizabeth A Bagshaw is an Associate Professor in Glaciology at the University of Bristol, UK. She specializes in instrument design for understanding water chemistry and microbial habitats in extreme cold environments.

Morgan L. Cable is the Science Lead of the EELS project and Co-Deputy PI of the Planetary Instrument for X-ray Lithochemistry (PIXL) instrument on the M2020 Perseverance rover. She has worked on the Cassini mission, is a Co-Investigator of the Dragonfly mission to Titan, and is serving multiple roles on the Europa Clipper mission. Morgan's research focuses on organic and biomarker detection through both in situ and remote sensing techniques. She earned her Ph.D. in Chemistry from Caltech in 2010.

Eddy Cartaya is the co-owner of Direct Action Vertical managing the field safety and rigging for the EELS project. He graduated West Point with a degree in aerospace engineering in 1990 and has been a leader in mountain, cave, arborist, and tactical rescue operations since. Currently the president of International Technical Rescue Association.

Guglielmo Daddi is a Ph.D. student in Politecnico di Torino's aerospace and mechanical engineering department and a visiting researcher at JPL focusing on Risk-Aware planning and software integration for the EELS project.

Rachel K. Etheredge is Deputy Project Manager for the EELS Project and served as JPL Field Commander and Media Capture Lead for the EELS Field Test at Athabasca Glacier. Her career focus lies in rapid development team management and strategic planning with a strong emphasis on whole team communications. Rachel also serves as Lead Producer for The Studio, a group of communications strategists and storytellers at NASA's Jet Propulsion Laboratory.

Alex S. Gardner is the Earth Science Lead of the EELS project. He studies the Earth's cryosphere (frozen Earth) with a particular focus on glaciers and ice sheets and their impacts on sea level rise and water resources. He earned his Ph.D. in Earth Science from the University of Alberta in 2010.

Bryson Jones is a Robotics Technologist in the Robotic Manipulation and Sampling Group at JPL. His research interests are in developing algorithms and robust software architectures that enable complex autonomous behaviors of robotic systems, especially through learning methods. Bryson received a M.S. in Robotic Systems Development from Carnegie Mellon University, where his worked focused on autonomy algorithm development for self-driving vehicles.

Michael J. Malaska is the Instrument Lead of the EELS project and the Deputy PI of the NASA Astrobiology Institute node studying the habitability of Saturn's moon Titan. Michael's research focuses on the surface geology of Titan and the exploration of microhabitats in Deep Ice on Earth and possibly the Ocean Worlds. He obtained his

PhD in Chemistry from the University of California, Berkeley in 1991. Before joining JPL in 2012, he spent 20 years in the pharmaceutical industry leading compound discovery/optimization efforts.

***Eloïse Marteau** is a Robotics Technologist in the Robotics Modeling and Simulations group at JPL. Her specialized interest lies in combining experimental, numerical, and analytical tools to study the mechanistic interactions between robotic systems and complex terrains, including extraterrestrial regolith and porous ice substrates. She holds a Ph.D. in Applied Mechanics from Caltech.*

***Martin Peticco** is a mechanical and aerospace engineer working as a Robotics Mechanical Engineer in the Extreme Environment Robotics Group at JPL. He began at JPL during his junior year of undergraduate studies, and his time on the EELS project has consisted of designing and building experimental testbed hardware to support the development of screw mobility. He completed his bachelor's in mechanical engineering and aerospace Engineering from the California Institute of Technology in 2023.*

***Rob Royce** is a Data Scientist at NASA's Jet Propulsion Laboratory (JPL), contributing to the Artificial Intelligence and Analytics group. His work involves a blend of Software Engineering, Artificial Intelligence/Machine Learning (AI/ML), Embedded Programming, and Robotics. Through collaborative efforts, he helps leverage data-centric solutions to address various aerospace challenges, aiding in the practical application of AI within various JPL projects.*

Christian Stenner is an explorer and cave rescue coordinator and holds an M.Sc. in organizational resilience. His research interests are in speleology, volcanology, resilience, and crisis management, with a recent focus on glaciovolcanic interactions that produce cave systems.

***Dr. L. Phillipe Tosi** is a mechanical and aerospace engineer working as a robotics technologist in the extreme environment robotics group at NASA's JPL, where he manages and contributes to robotics research projects including a long-lived Venus lander, a Mars deep drill, the Europa lander, and Mars flight technology. Phillipe has led industry-collaborative projects at JPL with the oil and gas sector, where he spent 9-year of his previous life as a completions engineer, project manager, and in research and development. He has a bachelors and master's in aerospace engineering from Cornell University, and a master's and doctorate in mechanical engineering from the California Institute of Technology, with the latter two focusing on fluid-structure interaction problems.*

***Michael R Prior-Jones** is a UKRI Future Leaders Fellow at Cardiff University. His research focusses on the development and deployment of low-cost open-source instrumentation for studying glacier hydrology. Before joining Cardiff University in 2019, he worked as an electronic and communications engineer in a variety of sectors, including spending a winter in Antarctica with the British Antarctic Survey. He obtained his PhD on polar radio communications from the University of Leicester in 2011.*

***Tony Tran** is a Business Analyst for the JPL Robotics Section (Section 347), supporting the business administration needs for numerous groups within Section 347. He also directly supports various robotic R&TD projects with field testing of experimental robotic hardware platforms, field safety, logistics, transportation, and field operations. Tony holds a Bachelors of Art in Film & Photography from the University of Minnesota.*

***Marcel Veismann** is a Robotics Mechanical Engineer in the Advanced Robotic Systems Group at JPL. He earned his Ph.D. in aeronautics from Caltech in 2022. Marcel's current research interest lies at the intersection of experimental fluid mechanics and robotics, with a focus on low Reynolds number multirotor aerodynamics and screw-based propulsion for snake-like robots. His previous research efforts further include novel multi-fan wind tunnel design concepts and active flow control technologies for advanced aircraft designs.*

***Harshad Zade** is a member of the EELS autonomy team at NASA's Jet Propulsion Laboratory (JPL), where he is an intern specializing in gait control and motion/path planning algorithms for the EELS snake robot. He also contributes to integration and hardware teams in a supplementary role. Harshad is currently pursuing an M.S. in Robotic Systems Development (MRSD) at Carnegie Mellon*

University, under the mentorship of Deepak Pathak and John Dolan.
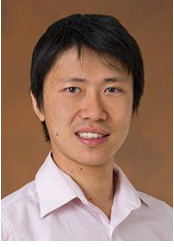
__Masahiro (Hiro) Ono__ is the Principal Investigator of the EELS project and the Group Supervisor of the Robotic Mobility Group at JPL. Previously, he developed M2020's autonomous driving algorithm and led the landing site traversability analysis. His research interest is centered around the application of robotic autonomy to space exploration, with an emphasis on machine learning applications to perception, data interpretation, and decision making. Before joining JPL in 2013, he was an assistant professor at Keio University in Japan. He graduated from MIT with PhD in Aeronautics and Astronautics in 2012.